Short Communication

The Effect of Morphology and Temperature on the Electrochemical Capacitive Performance of Mesoporous Carbons Synthesized Using Reverse Copolymers

Peng Li[1], Xiaoxiao Ma[1,2], Yanliang Zhao[1], Junhua Tan[1], Fei Liu[1], Kaijin Zhu[1]*

[1] Department of Materials Engineering, Taiyuan Institute of Technology, Taiyuan 030008, China
[2] Materials Science and Engineering School, North University of China, Taiyuan, 030051, China
[*]E-mail: nkpengli@nankai.edu.cn

Five kinds of mesoporous carbons (disordered mesoporous carbons (DMCs) which contain ink bottle (DMC-1) and cylinder structure (DMC-2), ordered mesoporous structure (OMCs) including lamellar (OMC-1), hexagonal (OMC-2) and cubic structure (OMC-3)) were selected to study the morphology and temperature on the electrochemical capacitive performance. Cyclic voltammetry and galvanostatic charging−discharging measurements are performed, and the results show that the OMC-2 has the best integrated electrochemical performance owning to synergistic effects of the hexagonal mesostructured and ordered pore arrangement. Moreover, the temperature on the pore structure and electric performance of DMCs was also studied, and the results show that too high temperature(1600°C) would result in disruption of pore structure which would further lead to the worse electric performance.

1. INTRODUCTION

To satisfy the high demand of energy requirements, several energy storage devices such as lithium or sodium battery, fuel cell battery, flow battery, lead acid battery and Electrical double layer capacitors (EDLCs) have been developed[1-3]. Among of them, EDLCs are one new type of the representative energy storage and devices that have advantages of high power density, high safety, environmental friendliness and convenient to operation over a wide temperature range[4, 5]. Porous carbons with controllable pore size, tunable pore structure[6, 7], surface area, low cost and easy handle have attracted numerous attention as the main components of the capacitors[8]. Mesoporous carbons(MCs), owing to their fascinating properties such as large pore volume, high surface area, tunable pore size, good conductivity and chemical ductility, have great potential for applications in a rapid

increasing range of fields: catalyst support[9, 10], pharmacy delivery and energy storage and conversion[11]. For EDLCs, MCs have their unique characteristics such as fast ion diffusion at high loading current density and efficient utilization of specific surface area when used as electrode materials[12]. Wu et al synthesized hierarchical porous carbons by pyrolysis and further activation based on Fir wood, and they found that that capacitive properties can be estimated by the BET surface area of porous carbons[13]. Xing et al prepared a series of ordered mesoporous carbons(OMCs) which contains hexagonal and cubic structure, and they found that OMCs with hexagonal structure not only provide high power density but also keep high energy density at the same time[14]. Liang et al also compared the electrocapacitive performance of OMCs with hexagonal mesostructure and DMC with disordered mesopore structure, they put emphasis on the contribution of pore morphology other than the pore size and insist that the pore morphology is a decisive factor[15]. Zhi et al prepared porous carbons derived from cycled waste tires and explore the effect of pore structure on the electrochemical performance for capacitor, and they found that the specific capacitance and rate capacity are dominated by the micropore volume and the ratio of mesopore/micropore, respectively[16].

Although much work has been done, the correlation between pore structure and electrochemical performance is not clearly understood. The aim of present work here is to explore the capacitance of mesoporous carbon with various pore size and pore structure. Therefore, five kinds of mesoporous carbons were prepared using the reverse triblock copolymer[17, 18].

2. ELECTROCHEMICAL MEASUREMENTS

Three-electrode configuration was used to measure electrochemical performance. Working electrodes were fabricated by the obtained samples between two pieces of circular nickel foams. A Pt-sheet and Hg/HgO electrode were used as the counter and reference electrodes, respectively. The working electrode was prepared as follows: a mixture of the as prepared sample, Super P and polytetrafluoroethylene (PTFE) at a weight ratio of 80:10:10 was prepared into film and then pressed between two nickel foams to form the working electrode. Cyclic voltammograms (CV), galvanostatic charge/discharge (current density from 0.1 to 5 A/g) and electrochemical impedance spectra (EIS, frequency range from 0.1 Hz to 100 kHz) were recorded on a CHI 760e electrochemical workstation. The 6M KOH aqueous solution was employed as the electrolytes. The specific gravimetric specific capacitance C (F/g) was calculated from the discharge process of the charge–discharge curve under different loading current density according to $C = It/mV$, where I is the constant discharge current (A), t is the discharging time, m is the mass of electrode and V is the potential window.

3. RESULTS AND DISCUSSION

3.1. Structural properties of the mesoporous carbons

Five kinds of MCs (ranging from cage-like, cylinder, lamellar, hexagonal to cubic) were selected

and their pore parameters are shown in table 1. From the table 1, it can be found that the BJH pore size have a wide range from 3.9 to 12.6 nm. Their pore volume varies 0.29 to 0.72 cm^3/g because of their distinctive pore size and structure, and their ratio of mesopore changes from 38% to 94% accordingly.

Table 1. Pore parameters of MCs

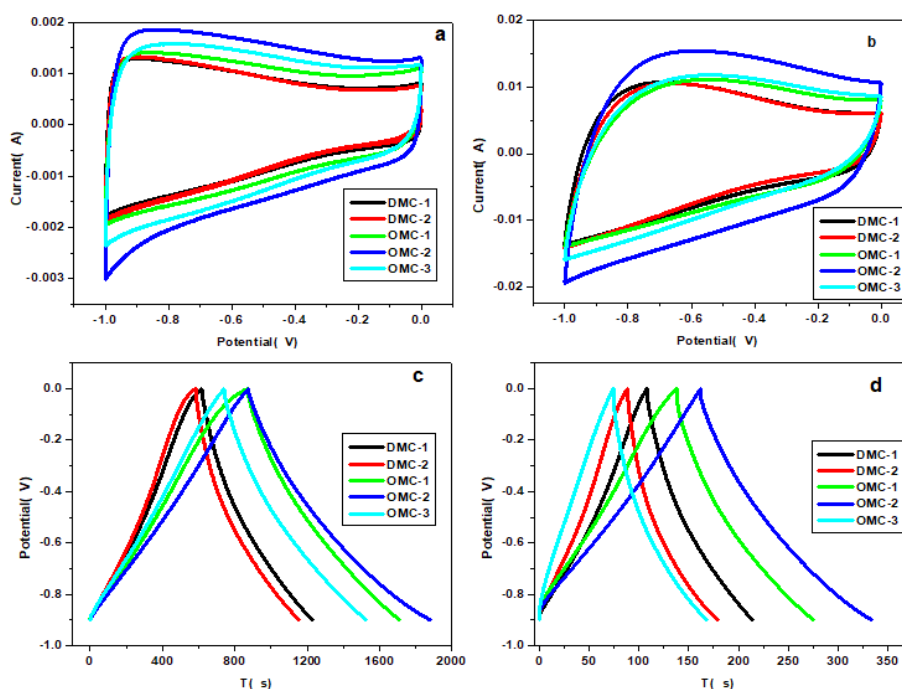| Sample	Pore structure	Pore size(nm)	S_{BET} (m^2/g)	V_{total} (cm^3/g)	V_{meso} (cm^3/g)	Ratio$_{meso}$ (%)
DMC-1	cage-like	5.5	389	0.34	0.27	71
DMC-2	cylinder	12.6	389	0.77	0.72	94
OMC-1	lamellar	6.7	472	0.29	0.11	38
OMC-2	hexagonal	3.9	503	0.38	0.20	53
OMC-3	cubic	3,4.8, 11.6	541	0.31	0.12	39

Ratio$_{meso}$=V$_{meso}$/V$_{total}$.

Figure 1. Cyclic voltammograms curves at various sweep rates and（a）5 mv/s, and（b）50 mv/s; charge−discharge curves at densities of (c) 0.1 A/g and（d）0.5A/g.

Fig.1a presents the CV curves of for five samples at a san rate of 5 mv/s, all samples show the near-rectangular shape which indicates that the almost ideal EDLC performance of samples[19, 20]. When the san rate increased to 50 mv/s, the rectangular shape almost could be kept which means that all

mesoporous samples had good rate capability as shown in Fig.1b. To further investigate the electrochemical performance of these samples, constant charge-discharge experiments were carried out. Fig.1c and d demonstrate the charge-discharge curves under current density of 0.1 and 0.5 A/g, respectively, symmetric charge and discharge curves and no any redox reaction observed confirmed the ideal EDLC performance furthermore[21]. The specific capacitances of DMC-1, DMC-2, OMC-1, OMC-2 and OMC-3 are 85, 80, 117, 140 and 109 F/g at current density of 0.1A/g and 73, 63, 95, 119 and 65 F/g at current density of 0.5A/g, respectively, which were consistent the CV results. OMC-2 exhibits the highest specific capacitance perhaps based on the synergistic effect the hexagonal mesostructure and ordered pore arrangement. Another interesting phenomenon is that OMC-3 has the high specific capacitance at current density of 0.1 A/g than that of the other samples at current density of 0.5 A/g. The reason is OMC-3 has the cubic mesostructure, and the ion moves slower under the lower current density and the ion has enough time to diffuse in the micropore. However, the ion transfers fast under the higher current density in which case they may block the transfer of ion. This phenomenon is also observed in the reported work as a shown in Table 2. The comparison was conducted by selecting similar structure as this work. It could conclude that the specific capacitance of OMC-2 are comparable to that of those reported OMCs [7, 12, 20].
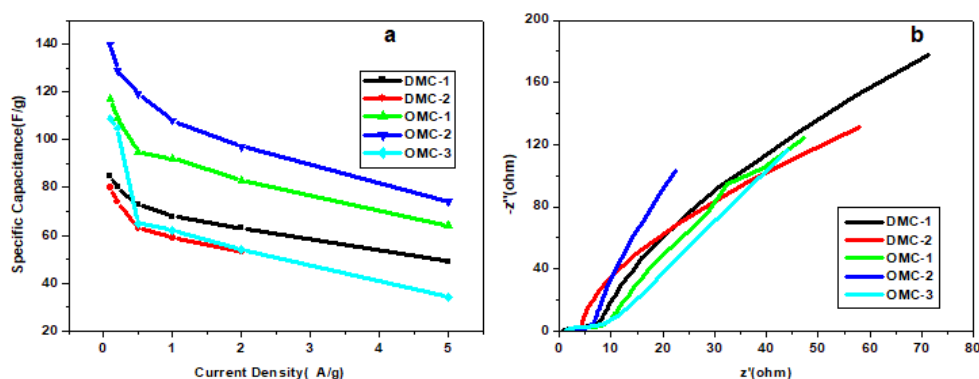

Figure 2. (a) Comparison of capacitance decay with increasing current densities for samples; (b) Nyquist plots of samples

Table 2. Comparison of specific capacitance with similar electrodes

Sample	Current density (A/g)	Specific capacitance (F/g)	pore structure	Ref.
FDU-15	0.5	130	Hexagonal	[20]
PCNS	0.2	83	Disordered	[7]
MCN-W	0.5	98	Hexagonal	[12]
OMC-2	0.1	140	Hexagonal	This work
OMC-2	0.5	119	Hexagonal	This work

The relationship current density vs specific capacitance is plotted in the Fig.2a. As can be seen in the Fig.2a, the specific capacitance value decreases gradually with the increasing current densities suggesting that less electrochemically active surface area of pores under higher current density. Similarly, the specific capacitance of the OMC-3 drops sharply than that of others. Specifically, all samples can retain more than 50% of their initial capacitance even at the current density of 5 A/g except the OMC-3(31%). The capacitive behaviors of these porous carbon samples were further studied by EIS with results shown in Fig. 2b. The interception of Nyquist curves with Z' axis at the high frequency represent the Ohmic resistance, which is the conductivity of the electrode[22]. The Ohmic resistance of DMC-1, DMC-2, OMC-1, OMC-2 and OMC-3 is about 0.8, 1.2, 2.2, 1.3 and 1.2 $\Omega \cdot cm^2$, respectively. The diameter of the semi-arc is used to analyze the charge transfer resistance, which is significant at high current density for capacitor. It can be seen that the OMC-3 has the largest diameter, which further explained that the worst rate capability and consistent with the rate performance shown in Fig2a.

Table 3. Pore parameters of samples under different temperatures

Sample	S_{BET} (m²/g)	V_{total} (cm³/g)	V_{micro} (cm³/g)	V_{meso} (cm³/g)	Ratio$_{meso}$ （%）
DMC-1	389	0.34	0.07	0.27	71
DMC-1-900	424	0.34	0.08	0.26	76
DMC-1-1200	545	0.36	0.13	0.23	64
DMC-1-1600	215	0.2	0.02	0.18	90
DMC-2	389	0.77	0.05	0.72	94
DMC-2-900	479	0.80	0.08	0.72	90
DMC-2-1200	453	0.72	0.09	0.63	88
DMC-2-1600	200	0.59	0.01	0.58	98

Ratio$_{meso}$=(V_{total}−V_{micro})/$V_{total.}$

The temperature on the electrochemical performance was also investigated, the DMC-1 and DMC-2 samples were carbonized at different temperature. The effect of the temperature on the parameters are listed in the table 3. It can be observed that both DMC-1 and DMC-2 have increasing surface area as the temperature increases. When the temperature reaches as high as 1600 °C, the surface area drops sharply possibly because of the disruption of pore structure. The ratio of mesopore volume and pore volume of DMC-2 are much higher that of DMC-1 due to the cylindrical straight pore.

Fig.3a, b, e, and f show the CV curves of DMC-1 and DMC-2 carbonization under different temperature at sweep rates 5 mv/s and 50 mv/s, respectively. It can be seen that all samples give near-rectangular curve at both sweep rates except for the DMC-1-1600 and DMC-2-1600, which can be ascribed to low surface area resulted by the disruption the pore structure shown in Table 2. The charge-discharge curves are demonstrated in Fig.3c, d, g and h, respectively. When the current density is 0.1 A/g, the specific capacitances increase from 85 to 92 F/g for DMC-1 and DMC-900, respectively. And then drops to 66 F/g when the temperature increases to 1200 °C. However, the specific capacitances of DMC-2, DMC-2-900 and DMC-2-1200 drop from 80 to 65 and increase to 79 F/g. The distinct phenomenon can be observed when the density is 0.5A/g, the specific capacitances of DMC-1, DMC-1-

900 and DMC-1-1200 are 73, 77, and 40 F/g. But for DMC-2, DMC-2-900 and DMC-2-1200 are 63, 60, and 59 F/g. Obviously, the DMC-1-1200 has relatively small capacitive value compared with that of DMC-2-1200, which can be ascribed to the straight pore of DMC-2-1200.
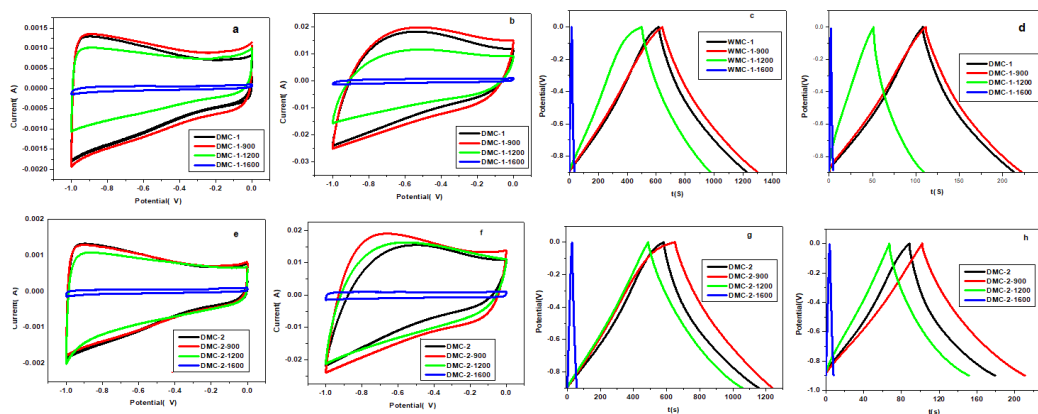

Figure 3. CV curves at various sweep rates (a)5 mv/s, and (b)50 mv/s and charge−discharge curves at densities of (c) 0.1A/g and （d） 0.5A/g for DMC-1 under different temperature; CV curves at various sweep rates(e)5 mv/s, and （f） 50 mv/s and charge−discharge curves at densities of (g) 0.1A/g and （h） 0.5A/g for DMC-2 under different temperature.

4. CONCLUSIONS

In summary, the effect of different pore morphology and temperature on the electrochemical performances of a series of porous carbons with cage-like, cylinder, lamellar, hexagonal and cubic are investigated. The electrochemical performances show that OMC-2 has the best specific capacitance (as high as 140 F/g at the density of 0.1A/g) compared with that of the other porous carbons owning the synergistic effects of pore morphology and ordered arrangement. Moreover, the effect of temperature shows that the suitable thermal treatment is beneficial to the specific capacitance, and too high temperature will damage to the pore structure which will lead to the lower specific capacitance.

References

1. L. Liu And Z. Niu, J. Chen, *Chem Soc Rev*., 45 (2016) 4340.
2. J. Pang, W. Zhang, H. Zhang, J. Zhang, H. Zhang, G. Cao, M. Han And Y. Yang, *Carbon*., 132 (2018) 280.

3. Y. Xu, C. Zhang, M. Zhou, Q. Fu, C. Zhao, M. Wu And Y. Lei, *Nat Commun.*, 9 (2018)1720.
4. R. Liu , L. Wan , S. Liu , L.Pan , D. Wu And D. Zhao, *Adv. Funct. Mater.*, 25 (2015) 526.
5. J. Wang, Y. Xu, B. Ding, Z. Chang, X. Zhang, Y. Yamauchi And K.C. Wu, *C Angew Chem Int Ed Engl.*, 57 (2018) 2894.
6. D. Zhou, Y. Du, Y. Song, Y.. Wang, C. Wang And Y. Xia, *J Mater Chem A.,* 1 (2013) 1192.
7. X. Yang, Z. Liang, Y. Yuan, J. Yang And H. Xia, *Acta Phys. Sin.*, 66 (2017) 048101.
8. M. Inagaki, M. Toyoda, Y. Soneda And T. Morishita, *Carbon.*, 132 (2018) 104.
9. Y. Zhang, A. Wang And T. Zhang, *Chem Commun.*, 46 (2010) 862.
10. P. Trogadas, T.F. Fuller And P. Strasser, *Carbon.*, 75 (2014) 5-42.
11. J. Lu, Z. Chen, Z. Ma, F. Pan3, L.A. Curtiss And K. Amine, *Nat Nanotechnol.*, 11 (2010) 1031.
12. M. Li And J. Xue, *J Colloid Interface Sci.,* 377 (2012) 169.
13. F. Wu, R. Tseng, C. Hu And C. Wang, *J Power Sources.*, 159 (2006) 1532.
14. W. Xing, S.Z. Qiao, R.G. Ding, F. Li, G.Q. Lu, Z.F. Yan, H.M. Cheng, *Carbon.*, 44 (2006) 216.
15. Y. Liang, Z. Li, X. Yang, R. Fu And D. Wu, *Chem Commun.*, 49 (2013) 9998.
16. M. Zhi, F. Yang, F. Meng, M. Li, A. Manivannan And N. Wu, *ACS Sustainable Chemistry & Engineering.*, 2 (2014) 1592.
17. P. Li, Y. Song, Q. Guo, J. Shi And Liu, *Mater Lett.*, 65 (2011) 2130.
18. P. Li, Y. Song, Q. Lin, J. Shi, L. Liu, L. He, H. Ye And Q. Guo, *Micropor Mesopor Mater.*, 159 (2012) 81.
19. D. Kang, Q.Liu, J. Gu, Y. Su, W. Zhang And D. Zhang, *ACSNANO.*, 9 (2015) 11225.
20. Y. Lv, F. Zhang, Y. Dou, Y. Zhai, J. Wang, H. Liu, Y. Xia, B. Tu And D. Zhao, *J. Mater. Chem.*, 22 (2012) 93.
21. H. Wang, L. Zhi, K. Liu, L. Dang, Z. Liu, Z. Lei, C. Yu And J. Qiu, *Adv Funct Mater.*, 25 (2015) 5420.
22. X. Xiao, C. Zhang, S. Lin, L. Huang, Z. Hu, Y. Cheng, T. Li, W. Qiao, D. Long, Y. Huang, L. Mai, Y. Gogotsi And J. Zhou, *Energy Storage Materials.*, 1 (2015) 1.